The effect of boron substitution for aluminium on the microstructure of calcium fluoro-aluminosilicate glasses and glass ceramics

Zhang, Siqi; Stamboulis, Artemis; Ni, Wen

DOI:
10.1016/j.jeurceramsoc.2018.11.023

Document Version
Peer reviewed version

Citation for published version (Harvard):
Zhang, S, Stamboulis, A & Ni, W 2018, 'The effect of boron substitution for aluminium on the microstructure of calcium fluoro-aluminosilicate glasses and glass ceramics', *Journal of the European Ceramic Society*. https://doi.org/10.1016/j.jeurceramsoc.2018.11.023

Title: The effect of boron substitution for aluminium on the microstructure of calcium fluoro-aluminosilicate glasses and glass-ceramics

Authors: Siqi Zhang, Artemis Stamboulis, Wen Ni

PII: S0955-2219(18)30688-5
DOI: https://doi.org/10.1016/j.jeurceramsoc.2018.11.023
Reference: JECS 12175

To appear in: *Journal of the European Ceramic Society*

Received date: 26 October 2018
Accepted date: 12 November 2018

Please cite this article as: Zhang S, Stamboulis A, Ni W, The effect of boron substitution for aluminium on the microstructure of calcium fluoro-aluminosilicate glasses and glass-ceramics, *Journal of the European Ceramic Society* (2018), https://doi.org/10.1016/j.jeurceramsoc.2018.11.023

The effect of boron substitution for aluminium on the microstructure of calcium fluoro-aluminosilicate glasses and glass-ceramics

Siqi Zhang [a,b], Artemis Stamboulis [a,*], Wen Ni [b]

[a] Biomaterials Group, School of Metallurgy and Materials, University of Birmingham, Edgbaston, Birmingham B15 2TT, UK

[b] School of Civil and Resource Engineering, University of Science and Technology Beijing, 30 Xueyuan Road, Haidian District, Beijing 100083, P.R. China

*corresponding author:a.stamboulis@bham.ac.uk

Abstract

Calcium fluoro-aluminosilicate ($4.5SiO_2$-$3Al_2O_3$-$1.5P_2O_5$-$3CaO$-$2CaF_2$) glasses have significant applications in the medical and dental fields. However, due to the biological hazard of aluminium in the human body, this study focused on the influence of boron substitution for aluminium on the structure and properties of a series of substituted glasses and their correlated glass-ceramics. The results indicated that by increasing the amount of boron, the density of glasses and their glass-ceramics both decreased, whereas the number of bridging oxygens in the glasses increased. The glass transition temperature and the crystallization temperature remained almost unchanged for the glasses with a boron substitution of less than 25 mol%. Boron formed oxygen bridges in all glasses in the form of BO_3 triangles and BO_4 tetrahedra. Reducing the Al content in glasses, had an effect on the morphology and orientation of the fluorapatite crystal phase formed.

Key words: Boron-Substitution, Calcium fluoro-aluminosilicate glasses, Fluorapatite, Mullite

1. Introduction

Fluoride containing calcium aluminosilicate glass can lead to glass ceramics with a fluorapatite phase which is a more stable phase compared to hydroxyapatite and can enhance bonding strength with the surrounding bone tissue as well as the remineralisation process[1]. Freeman et al. [2] reported that calcium fluoro-aluminosilicate glasses are able to crystallize into apatite and mullite phases to form apatite-mullite glass-ceramics, which showed excellent osteointegration and osteo-conduction properties when implanted in the human body. Dumini et al in their recent review provided a comprehensive account of the formation of apatite-mullite glass ceramics summarising all the most important findings about the apatite-mullite glass systems and glass ceramics [3]. Nearly all the commercially available glass used for dental cements is aluminosilicate glass based with some fluorine addition. However, long time service of fluoro-aluminosilicate glasses and alumina-containing glass-ceramics may lead to the release of aluminium ions, causing serious hazard to the human body despite some reassuring evidence provided in the literature that aluminium is not released to the surrounding tissue [4]. For example, Renard et al. [5] reported that in 1994 after bone reconstitution using Ionocem® IONOS-D8031 Seefeld/Obb, Germany, a glass polyalkenoate cement) a subacute Al myoclonic encephalopathy occurred. In the same year, in Belgium, Hantson et al. [6] reported two other cases of Al encephalopathy, which both led to death.

Bladed et al. [7] reported that the glass ionomer cements with low aluminium release from the unset cement matrix, and the release of aluminium from the set cement restricted the mineralization of osteoid and remineralisation of bone. It is expected, that the reduction of aluminium contents with a more closely packed glass-network could decrease the releasing amount of aluminium ions from the glass. As a glass former, boron trioxide

(B_2O_3) can increase the chemical resistance of the glass and can be a possible substitute for aluminium to reduce the aluminium content in glass [8]. As it was known in normal glass network, Al normally can form Al-O bonds with oxygen, however, by introducing fluorine ions, considerable fractions of network Al-O bonds are replaced by weaker non-network Al-F bonds [9], indicating that fluorine could disrupt the glass network by substituting bridging oxygens with non-bridging fluorines [10,11]. Stamboulis et al. [12] reported that Si-F-Ca(n) species were clearly present in fluoro-aluminosilicate glasses, with the general composition of $4.5SiO_2$-$3Al_2O_3$-$1.5P_2O_5$-(5-x)CaO-$xCaF_2$, where x equals to 0-3. Therefore, fluorine ions may increase the possibility of boron to replace aluminium ions in the glass network with the formation of B–O bonds thus changing the type of the crystallization phase in a fluoro-aluminosilicate ceramic.

This study focuses on the effect of boron substitution for aluminium on the structure of fluoro-aluminosilicate glasses and glass ceramics.

2. Materials and methods

2.1 Preparation of materials

The molar composition of calcium fluoro-aluminosilicate glasses are shown below in Table1. Powders of silicon dioxide (SiO_2, Sigma-Aldrich, purum p.a. powder), aluminium oxide (Al_2O_3, Sigma-Aldrich, puriss powder), phosphorus pentoxide (P_2O_5, Sigma-Aldrich, puriss powder), calcium fluoride (CaF_2, Sigma-Aldrich, natural powder), boron oxide (B_2O_3, Sigma-Aldrich, 99%(after heating)), and calcium carbonate ($CaCO_3$, Sigma-Aldrich, BioXtra) were firstly mixed by hand-shake for 30 min, and then transferred to a platinum rhodium (Pt, 5% Rh) crucible. The crucible was then placed into an electric furnace (EHF 17/3, Lenton, UK) under a temperature of 1450 ºC for 1.5 h. The

glass melt was then water quenched to prevent phase separation and crystallisation. All of the glasses were finally milled using a gyro mill to very fine particles (<45 μm) [13].

2.2 Crystallisation of FB0, FB25 and FB50 glasses

Three glass compositions FB0, FB25 and FB50 were selected for crystallisation studies. 2 g of glass powder (<45 μm) were pressed into a die to produce test tablets for the heat treatment. The tablets were then placed to a platinum crucible in an electric furnace (EHF 17/3, Lenton, UK). The samples were first heated to 700 °C with a heating rate of 10 °C /min, held for 1 h for nucleation, and then heated up to 1100 ° C at the same heating rate, holding for 1 h for crystallisation and finally furnace cooling to room temperature.

2.3 Characterisation of glasses and glass-ceramics

The thermal transitions of glasses were analysed using differential scanning calorimetry (Netzsch 404C DSC) along with pairs of matched platinum-rhodium crucibles. Every sample powder was weighed to around 20 mg for each run. The samples were firstly heated to 1200 ºC with a heating rate of 10 ºC /min and then air cooled. The glass transition (T_g) and peak crystallisation temperatures (T_p) were identified.

Thermogravimetric analysis (TGA) is normally used to test the weight change of materials at different temperatures, which was usually used to measure the weight loss of the material during heat-treatment. In this experiment, a TGA (Netzsch 404C STA) was used with the pairs of matched platinum-rhodium crucibles, and all the tests were carried out under a dry argon environment at a heating rate of 10 ºC /min.

The densities of all samples were identified using an AccuPyc II 1340 Series Helium Pycnometer. The gas pycnometry uses a glass displacement method to test the sample volume. The glass weight was 1 g. In order to calculate the density of the glasses and glass-ceramics, an average of 10 consecutive measurements was taken. The oxygen density (OD) of each glass was calculated by using the following equation:

$$OD = D \times \frac{No.\ of\ moles\ of\ oxygens\ in\ the\ glass}{molecular\ weight\ of\ glass} \qquad \text{(Equation 1)}$$

where D is the density of the glass measured by the helium pycnometer.

The glasses were further characterised by Fourier Transform Infrared Spectroscopy (FTIR, Spectrum2000, PerkinElmer, USA). A 1:100 wt ratio between the sample and potassium bromide (KBr) was used to obtain the spectra. The background of the test trace was always taken by using a control sample of KBr prior to each measurement. A diffuse reflectance accessory was used to obtain a spectrum from 400–4000 cm^{-1} wavenumbers with the resolution of 4 cm^{-1} and 100/min number of scans.

The glass-ceramics were also characterised by X-ray diffraction using a continuous scan between $2\theta = 10°$ and 90°, with a step size of $2\theta = 0.0200°$ in a Philips analytical X-Pert XRD at the University of Birmingham with a Cu Ka, at 40 kV and 40 mA, and a MAC Science Co. Ltd M21X XRD at the University of Science & Technology Beijing with Cu Ka, at 40 kV and 130 mA.

^{11}B MAS-NMR analysis was conducted at resonance frequencies of 128.07 MHz, using a Bruker ADVANCE 400 III Solid-state NMR spectrometer. The magnetic field was 9.4 T, the spinning rates of the samples at the magic angle was 12 KHz. The delay time was 1 s.

The reference material used was $BF_3 \cdot OEt_2$ for ^{11}B. ^{11}B peaks were observed at around 0.5 ppm and 9 ppm, which are assigned to BO_4 tetrahedra and BO_3 triangles [14].

An XL 30 ESEM&EDX FEG scanning electron microscope operated at 20 kV was used to investigate the morphology changes of the glasses under different heat treatment temperatures. Energy Dispersive Spectrometer (EDS) was used to study the composition of the different phases. The analysis took place under high-vacuum conditions. Prior to characterization all glass-ceramics were etched with 10% HF and the samples were coated with carbon using an SB250 coating machine.

3. Results

3.1 The change of microstructure and property of glass

3.1.1 Density

The changes of density in glasses and their glass-ceramics are shown in Figure 1(a). As can be seen, the glass without boron substitution had the highest density even after its sintering. By increasing the amount of boron substitution, the density of glass decreased proportionally from FB0 (2.768 g/cm^3) to FB50 (2.695 g/cm^3) glass, showing a linear relationship between the density and boron molar content in each glass. The oxygen density of glasses shown in Figure 1(b) suggested that boron substitution for aluminium resulted in increased oxygen density from 0.0709 mol/cm^3 to 0.0721 mol/cm^3 leading to a slightly more compact glass network.

3.1.2 FTIR

The FTIR spectra for boron-substituted glasses and glass-ceramics are shown in Figure 2. As can be seen, from the FB0 to FB25 boron-substituted glasses, the main broad

absorption did not change significantly. Only very broad bands appeared in the region between 800 and 1200 cm^{-1} indicating the presence of Si-O(s) stretching vibrations with different number of bridging oxygens and P-O bonds [15]. For the boron substituted glass, a small peak appeared in the region between 1200 and 1600 cm^{-1} (marked in the spectra by a red rectangular), indicating the presence of B-O stretching vibrations in BO_3 units [16-20]. However, in the case of the 50 mol% Al containing FB50 glass, some very weak peaks appeared at 460 cm^{-1}, 567 cm^{-1},602 cm^{-1}, 720 cm^{-1},1038 cm^{-1},1093 cm^{-1},1277 cm^{-1} and 1400 cm^{-1} suggesting that the FB50 glass was partially crystallised, with the most intense absorption bands at 1038 cm^{-1} due to the asymmetric stretching vibrations (P-O, v_3) of phosphate tetrahedra with four non-bridging oxygens (NBOs) (PO_4). It is clear, that the P-O peak in the FB50 glass ceramic was the result of two bonding vibrations at 602 and 576 cm^{-1} corresponding to the O-P-O bending vibrations of phosphate groups (v_4) and are characteristic of an apatite crystal phase. The peak at 729 cm^{-1} was associated with the presence of Al-O (AlO_4) [21, 22].

3.1.3 Glass transition and crystallisation temperatures of substituted glasses

In Figure 3 and Table 2, boron-substituted glasses showed that the glass transition temperatures (T_g) of FB0 to FB15 samples appeared in the region from 656 to 647ºC. With increasing boron substitution to 25 mol%, a significant decrease of T_g was observed from 648 ºC (FB15) to 605 ºC (FB25). Meanwhile in the case of FB50, T_g was slightly increased due to the partial-crystallisation of the glass during the production of the glass. By increasing the amount of boron substitution, the first crystallisation temperature of glasses decreased from 741ºC (FB0) to 636 ºC (FB25). In the case of FB50, the first crystallisation temperature was slightly higher. Compared to the first crystallisation temperature, the change of the second crystallisation temperature of glasses showed a

similar trend. The highest second crystallisation temperature was observed for FB15 and was 1089 ^{o}C, while in the case of FB25, three crystallisation temperatures were observed. It is important to mention, that FB25b did not crystallise during the glass production exhibiting the lowest T_g, T_{p1}, T_{p2}, and T_{p3}. It can be observed that there was a decreasing tendency in T_{p1} and T_{p2} by increasing the content of boron substitution for aluminium in the glasses.

3.1.4 XRD study of substituted glasses

Figure 4 shows the main crystal phases observed by X-ray diffraction for FB0, FB25 and FB50 glasses and glass-ceramics at a heating rate of 10^{o}C/min. It can be clearly seen, that FBO and FB25 did not have any peak present in their X-ray diffractograms indicating that the glasses were both amorphous. However, FB50 exhibited some sharp peaks suggesting clearly formation of fluorapatite ($Ca_5(PO_4)_3F$).

3.2 The bonding structure and microstrucure of boron-substituted glass-ceramics

To better understand the effect of boron on the structure of glass-ceramics, ^{11}B MAS–NMR was used to study the bonding changes before and after crystallization of glasses [23]. The results are shown in Table 3 and Figure 5.

As reported by H. Miyoshi [24], the chemical shift of BO_3 species should be around 8.56 ppm, whereas the chemical shift around 0.9-1.7 ppm is ascribed to the BO_4 unit [25]. ^{11}B MAS–NMR spectra showed the appearance of two main peaks at around 0.2-0.8 ppm and 9.0-9.5 ppm, which were associated with BO_4 and BO_3 species, respectively. From the ^{11}B MAS–NMR spectra of boron-substituted glasses and glass-ceramics in Figure 5, all samples exhibited peaks at 0.5 and 9.0 ppm, assigned to BO_4 and BO_3 species, respectively. There was also no change in the bonding with increasing boron substitution

for aluminium, suggesting that the boron atoms were stable in the form of BO_4 and BO_3 groups in the glasses. Initially, due to the smaller cation size of boron ion, it was thought that boron may have acted as a network former, taking up a four-fold coordination and forming BO_4 structural units. Boussard-Plédel and Floch reported that a peak at 33 ppm in the ^{19}F spectra (0 ppm for C_6F_6) and a peak at 12 ppm in the ^{11}B (0 ppm for Et_2OBF_3) spectra of a boron oxyfluoride glass corresponded to the resonance position of the respective nuclei in the BF_3 species present above the glass Tg (320K) [26]. In our case however, the glasses did not exhibit the peak at 12 ppm in the ^{11}B MAS-NMR spectra suggesting the absence of BF_3 species, possibly escaped as a gas during glass preparation.

A high absorbance between 400 cm^{-1} and 1400 $cm^{-1}$was observed in the FTIR spectra of glasses shown in Figure 6 indicating mainly the formation of Si-O-Si, Si-O-Al, P-O and Al-O bonds. The intensity of the absorption bands centred at 1170 cm^{-1} increased with boron substitution, while the bands shifted from 1097 cm^{-1} in FB0 to 1170 cm^{-1} in FB50, suggesting the transformation of $[SiO_{1/2}O_3]^{3-}$ to $[SiO_4]^{4-}$ with increasing boron substitution for aluminium [27] . The absorption bands centred at 1082 cm^{-1}were attributed to the asymmetric stretching vibrations (P-O, ν3) of phosphate tetrahedra, and the bands at 977 cm^{-1}, 963 cm^{-1}, and 950 cm^{-1}were attributed to the symmetric stretching vibrations of phosphate (ν1) species [21,28]. Two bands at 576 cm^{-1} and 605 cm^{-1} were attributed to the O-P-O bending vibrations of phosphate (ν4) species, whereas the band centred at 450 cm^{-1} was associated with the phosphate (ν2) bending vibrations [22].

Besides, the X-ray diffractogramms, shown in Figure 7, suggested that the crystal phases present in the boron free FB0GC glass ceramic were fluorapatite ($Ca_5(PO_4)_3F$) and mullite ($Al_6Si_2O_{13}$) with a small amount of aluminium phosphate ($AlPO_4$). However, for FB25 GC and FB50 GC, the intensity of mullite and aluminium phosphate decreased with increasing boron substitution for aluminium as it was expected. In the case of FB50 GC,

mullite and aluminium phosphate were only minor crystal phases. Furthermore, the peak of the fluorapatite phase did not change much in all boron substituted fluoro-aluminosilicate glass-ceramics, suggesting that by the addition of boron, no new phases appeared.

The morphology and compositions of boron-substituted glass and glass-ceramics is presented in Figure 8 and Table 4. All samples showed the presence of needle-like bright phases, surrounded by a dark phase. EDX analysis showed that the needle-like phase identified as fluorapatite phase, contained mainly F, P, and Ca, whereas the dark phases, contained high amount of O, Al, Si and a small amount of P and were assigned to the mixture of mullite and $AlPO_4$ phases. By increasing the boron content, the crystallisation of the fluorapatite phase was generally promoted. More importantly, after high amount of substitution, e.g. FB25 and FB 50, the growth direction of the needle-like fluorapatite crystals changed from random to oriented, in which multiple needle-like crystals with the same orientation became one cluster with an average size of around 100μm.

4. Discussion

In this study, a new type of biocompatible glasses were developed by partially substituting aluminium by boron. The densities of glasses gradually decreased with increasing boron substitution (Table 2, Figure 1). The change in the density of glasses was due to the different atomic weight of boron and aluminium atoms, e.g. boron has lighter atomic weight (AW = 10.81) than aluminium (AW = 26.98). In addition, the ionic radius of four fold-coordinated B(III) (tetrahedral) is 25 pm and the ionic radius of six fold-coordinated B(III) (octahedral) is 41 pm, both shorter than the ionic radius of four fold-coordinated Al(III) (tetrahedral, 53 pm) and six fold-coordinated Al(III) (octahedral, 67.5 pm). Therefore, the replacement of aluminium with boron resulted in a more compacted

network with increased density. In this study, a decrease in the density of glasses was observed with increasing boron substitution, indicating that the change of the atomic weight had a more significant effect on the density of glasses than the ionic radius. A linear increase in the oxygen density with increasing boron substitution was observed in Figure 1b, indicating a closer packed glass network [29, 30].

Besides the effect on the density of glasses, boron substitution caused also changes in the glass transition and the crystallisation temperatures of glasses (Figure 2 and Table 3). The glass transition temperature of glasses decreased with increasing boron substitution. For example, in the case of FB0 and FB15 glasses, the glass transition temperature was stable and around 650ºC. For FB25 glass, however, the glass transition temperature was observed at a much lower temperature at 605ºC. This observation is in agreement with Hill *et al* [31]. Similarly, the crystallization temperature of glasses decreased with increasing boron substitution. For example, the first crystallisation temperature was decreased from 741ºC (FB0) to 643ºC (FB50, partially crystallised), while FB15 and FB25 glasses had the highest and the lowest T_{p2}, respectively. In the case of FB25 glass, a third crystallisation peak was observed at 946ºC, suggesting that the second crystallisation peak separated in two parts: one corresponding to fluorapatite formation, and another smaller peak most likely corresponding to the aluminium phosphate formation in agreement with Rafferty et al. [32]. The FB50 glass crystallised during glass formation evidenced by the X-ray diffractogram shown in Figure 4.

Decreasing the amount of aluminium in the glass composition, had a significant effect on the silicate species formation in the glass network. A transformation from $[SiO_{1/2}O_3]^{3-}$ to $[SiO_4]^{4-}$ was observed with increasing boron substitution in agreement with the literature [27]. A strong effect was observed also in the case of phosphorous containing species. For

example, increasing boron substitution resulted in changes in the absorption bands of stretching vibrations (P-O, ν3) of phosphate tetrahedral split from one peak at 1082 cm^{-1}into two peaks at 1045 $cm^{-1}$and 1097 cm^{-1}, respectively. The change of the proportion of chemical elements in the glasses with boron substitution, lead to the formation of different crystal phases in the glass-ceramics from the formation of $AlPO_4$, $Al_6Si_2O_{13}$ and $Ca_5(PO_4)_3F$ in the case of FB0 to the formation of a dominant $Ca_5(PO_4)_3F$ phase and a minor $Al_6Si_2O_{13}$ phase in the case of F50. Boron, as a glass former was present as BO_4 and BO_3 species in all glasses as it can be seen in the FTIR and NMR results shown in Figures 2 and 5.

Due to the lack of a boride based crystal phase, boron could be present in the glass-ceramics as solid-solution in $Ca_5(PO_4)_3F$ and $Al_6Si_2O_{13}$. This could potentially lead to a change for example in the hydroxyapatite lattice parameters as evidenced with the shifting of the characteristic peaks in the X-ray diffractograms with addition of boron shown in Figure 4. A characteristic preferential orientation of fluorapatite crystals was observed by SEM shown in Figure 8 when boron addition was larger than 15 mol%. This is very difficult to explain with the data presented in this study. However, previous studies on apatite-mullite glasses concluded that the main mechanism of crystallisation is amorphous separation and nucleation [33]. The addition of boron may have resulted in a decrease of the crystallization temperature of the glass. Amorphous phase separation may have been occurred [3, 34] and consequently, during crystallisation, fluorapatite crystals would preferentially precipitate by heterogeneous nucleation on the pre-existed crystals that as a result allowed the formation of needle-like clusters with similar orientation. Hoeland *et al* [35] stated clearly that in the case of a leucite-apatite glass ceramic, the superfast growth of fluorapatite crystals, caused by heterogeneous nucleation, could alter the growth behaviour and orientation of fluorapatite crystals. Further work is required to understand

the role of boron to the growth and orientation of fluorapatite crystals, if it is present as solid solution.

5. Conclusions

The density of both boron-substituted for glasses and glass-ceramics decreased with increasing boron substitution for aluminium. The oxygen density of all substituted glasses increased slightly with increasing boron substitution for aluminium, which suggested the formation of a more compact glass network. The glass transition temperature remained stable in boron-substituted for aluminium glasses when boron substitution was lower than 25 mol%. Higher amount of boron substitution (>25 mol%) for aluminium lead to a decrease of both glass transition and crystallization temperatures, resulting in fluorapatite crystallization during the formation of glass network. Boron atoms in the glasses were present as BO_4 triangles and BO_3 tetrahedra. There is no change of morphology for the fluorapatite phase in the glass-ceramics when boron substitution was not in excess of 15mol%. High amount of boron substitution resulted in the change of fluorapatite crystal growth behaviour by forming highly oriented clusters as evidenced by SEM. However, more work is required to understand the role of boron on the crystallisation mechanism and morphology.

Acknowledgments

The authors would like to thank Ningning Wu of the Institute of Chemistry, Chinese Academy of Sciences for her assistance with the solid-state ^{11}B NMR study.

References

[1] T. De Caluwé, C. W. J. Vercruysse, "Bioactivity and biocompatibility of two fluoride containing bioactive glasses for dental applications." *Dental Materials* vol. 32, pp. 1414-

1428, 2016.

[2] C. O. Freeman, I. M. Brook, A. Johnson, P. V. Hatton, K. T. Stanton, R. G. Hill, "Crystallization modified osteoconductivity in an apatite-mullite glass-ceramic". *Journal of Materials Science: Materials in Medicine*, vol. 14, pp. 985-990, 2003.

[3] T. Duminis, S. Shahid, R.G. Hill, "Apatite Glass-Ceramics: A Review". *Frontiers in Materials*, vol. 3, article 59, 2017

[4] R.A. Martin, Z.Jaffer, G. Tripathi, S. Nath, M. Mohanty, V. FitzGerald, P. Lagarde, A.-M. Flank, A. Stamboulis, B. Basu, "An X-ray micro-fluorescence study to investigate the distribution of Al, Si, P and Ca ions in the surrounding soft tissue after implantation of a calcium phosphate-mullite ceramic composite in a rabbit animal model". *Journal of Materials Science: Materials in Medicine*, Vol. 22(11), pp. 2537-2543, 2011

[5] J. L. Renard, D. Felten, D. Bequet, "Post-otoneurosurgery aluminium encephalopathy". *Lancet* 344:63, 1994

[6] P. H. Hantson, M. Mahieu, M. Gersdorff, "Encephalopathy with seizures after use aluminium-containing bone cement". *Lancet* 344:1647, 1994

[7] M. C. Blades, D. P. Moore, P. A. Revell, R. Hill, "In vivo skeletal response and biomechanical assessment of two novel polyalkenoate cements following femoral implantation in the female New Zealand White rabbit." *Journal of Materials Science: Materials in Medicine*, vol. 9:70, pp. 1–6, 1998

[8] M. Bengisu, R. K. Brow, *Journal of Non-Crystalline Solids*, vol. 352, pp. 3668-3676, 2006.

[9] Q. Zeng and J. F. Stebbins, "Fluoride sites in aluminosilicate glasses: High-resolution F-19 NMR results", *American Mineralogist*, vol. 85, pp. 863-867, 2000.

[10] A. D. Wilson, S. Crisp, H. J. Prosser, B. G. Lewis, and S. A. Merson, "Aluminosilicate

glasses For Poly-Electrolyte Cements", *Industrial & Engineering Chemistry Product Research And Development*, vol. 19, pp. 263-270, 1980.

[11] R. G. Hill and A. D. Wilson, "Some structural aspects of glasses used in ionomer cements", *Glass Technology*, vol. 29, pp. 150-157, 1988.

[12] S. Matsuya, A. Stamboulis, R. G. Hill, and R. V. Law, "Structural characterisation of ionomer glasses by multinuclear solid state MAS-NMR spectroscopy," *Journal of Non-Crystalline Solids*, vol. 353, pp. 237-243, 2007.

[13] Siqi Zhang, A. Stamboulis, "Effect of zinc substitution for calcium on the crystallisation of calcium fluoro-alumino-silicate glasses." *Journal of Non-Crystalline Solids*, vol. 432, Part B: pp. 300-306, 2016.

[14] B. C. Bunker, ,R. J. Kirkpatrick, R. K. Brow, G. L. Turner and C. Nelson, *Journal of The American Ceramic Society*, vol. 74, pp. 1430, 1991.

[15] S. A. MacDonald, C. R. Schardt, D. J. Masiello, and J. H. Simmons, "Dispersion analysis of FTIR reflection measurements in silicate glasses," *Journal of Non-Crystalline Solids*, vol. 275, pp. 72-82, 2000.

[16] R. Iordanova, V. Dimitrov, Y. Dimitriev, and D. Klissurski, "Glass formation and structure of glasses in the V_2O_5 -MoO_3 -Bi_2O_3 system", *Journal of Non-Crystalline Solids*, vol. 180, pp. 58-65, 1994.

[17] Y. D. Yiannopoulos, and G. D. Chryssikos, "Structure and properties of alkaline earth borate glasses", *Physics and Chemistry of Glasses*, vol. 42, pp. 164-172, 2001.

[18] P. Pascuta, L. Pop, S. Rada, M. Bosca, and E. Culea, "The local structure of bismuth borate glasses doped with europium ions evidenced by FT-IR spectroscopy", *Journal of Materials Science: Materials in Electronics*, vol. 19, pp. 424-428, 2008.

[19] E.I. Kamitsos, M.A. Karakassides, and G.D. Chryssikos, "Vibrational spectra of magnesium-sodium-borate glasses. 2. Raman and mid-infrared investigation of the

network structure", *The Journal of physical chemistry*, vol. 91 (5), pp. 1073-1079, 1987.

[20] J. Krogh-Moe, "The structure of vitreous and liquid boron oxide", *Journal of Non-Crystalline Solids*, vol. 1, pp.269-284, 1969.

[21] R. N. Panda, M. F. Hsieh, R. J. Chung, and T. S. Chin, "FTIR, XRD, SEM and solid state NMR investigations of carbonate-containing hydroxyapatite nano-particles synthesized by hydroxide-gel technique," *Journal Of Physics And Chemistry Of Solids*, vol. 64, pp. 193-199, 2003.

[22] S. Haque, I. Rehman, and J. A. Darr, "Synthesis and characterization of grafted nanohydroxyapatites using functionalized surface agents," *Langmuir*, vol. 23, pp. 6671-6676, 2007.

[23] J. M. Oliveira, R. N. Correira, M. H. Fernandes, and J. Rocha, "Influence of the CaO/MgO ratio on the structure of phase separated glasses: a solid state 29Si and 31P MAS-NMR study," *Journal of Non-Crystalline Solids*, vol. 265, pp. 221-229, 2000.

[24] H. Miyoshi a, D. Chen a, H. Masui a, T. Yazawa c, T. Akai, "Effect of calcium additive on structural changes under heat treatment in sodium borosilicate glasses", *Journal of Non-Crystalline Solids*, vol. 345&346, pp. 99–103, 2004.

[25] B. C. Bunker, ,R. J. Kirkpatrick, R. K. Brow, G. L. Turner and C. Nelson, *Journal of The American Ceramic Society*, vol. 74, pp. 1430, 1991.

[26] C. Boussard-Plédel, M. Le Floch, "The structure of a boron oxyfluoride glass, an inorganic cross-linked chain polymer", *Journal of Non-Crystalline Solids*, vol. 209, pp. 247-256, 1997.

[27] K. El-Egili, "Infrared studies of Na_2O-B_2O_3-SiO_2 and Al_2O_3-Na_2O-B_2O_3-SiO_2 glasses", *Physica B: Condensed Matter*, Vol. 325, pp.340-348, 2003

[28] B. Sreedhar, M. Sairam, D. K. Chattopadhyay, and K. Kojima, "Preparation and

characterization of lithium fluorophosphate glasses doped with MoO_3," *Materials Chemistry And Physics*, vol. 92, pp. 492-498, 2005.

[29] R. Hill, D. Wood, and M. Thomas, "Trimethylsilylation analysis of the silicate structure of fluoro-alumino-silicate glasses and the structural role of fluorine", *Journal of Materials Science*, vol. 34, pp. 1767-1774, 1999.

[30] Fei Wang, Cation substitution in ionomer glasses: effect on glass structure and crystallization, PhD thesis (2009), University of Birmingham.

[31] M. D. Ingram, C. T. Imrie, and I. Konidakis, "Activation volumes and site relaxation in mixed alkali glasses," *Journal of Non-Crystalline Solids*, vol. 352, pp. 3200, 2006.

[32] A. Rafferty, A. Clifford, R. Hill, D. Wood, B. Samuneva, and M. Dimitrova-Lukacs, "Influence of fluorine content in apatite-mullite glass ceramics," *Journal of the American Ceramic Society*, vol. 83, pp. 2833-2838, 2000.

[33] MD O'Donnell, N Karpukhina, A. Calver, R.V. L:aw, N. Bubb, A. Stamboulis, R.G. Hill, Real time neutron diffraction and solid state NMR of high strength apatite –mullite glass ceramic, Journal of Non-Crystalline Solids, Vol. 356 (44-49), pp. 2693-2698, 2010

[34] A. Clifford and R. Hill, "Apatite-mullite glass-ceramics," *Journal of Non-crystalline Solids*, vol. 196, pp. 346-351, 1996

[35] W. Höland, and V. Rheinberger, "Control of nucleation in glass ceramics." *Philosophical Transactions of the Royal Society of London. Series A: Mathematical, Physical and Engineering Sciences*, 361 (1804): 575, 2003

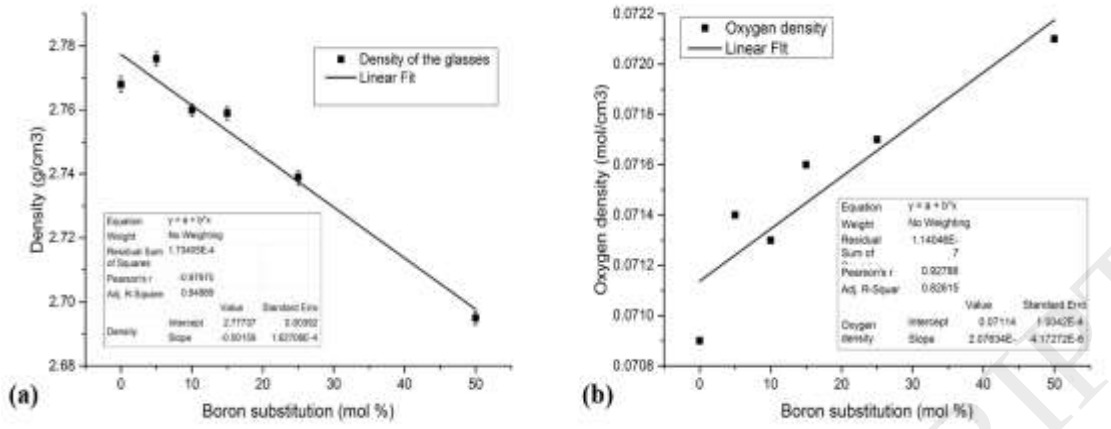

Figure 1: (a) Density and (b) oxygen density of the fluoro-aluminosilicate glasses.

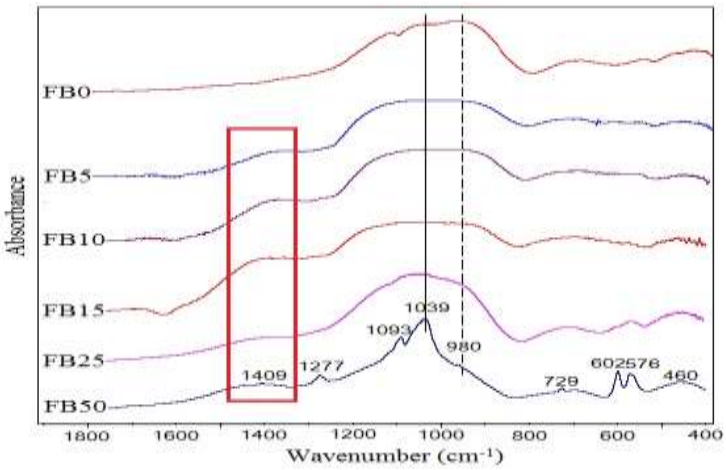

Figure 2: FTIR spectra of boron-substituted fluoro-aluminosilicate glasses.

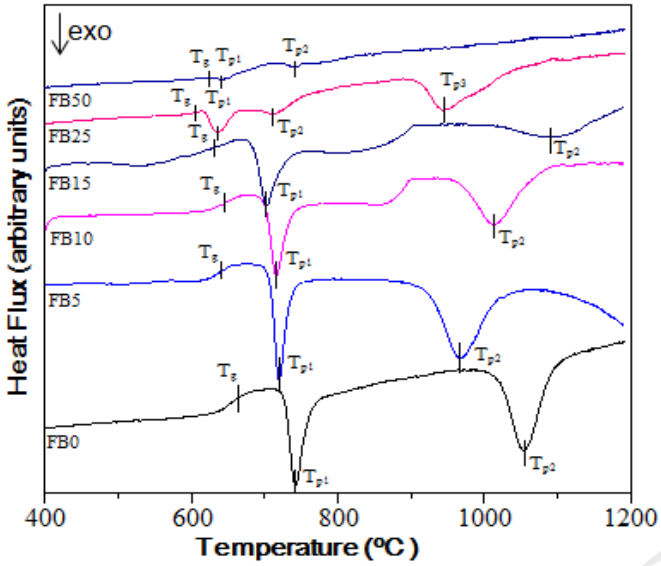

Figure 3: DSC trace of boron-substituted fluoro-aluminosilicate glasses at a heating rate of 10ºC/min.

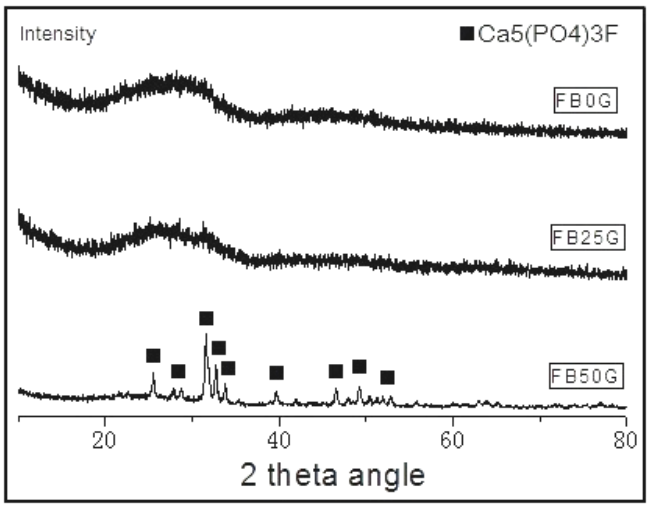

Figure 4: XRD results of FB0, FB25, and FB50 boron-substituted glasses.

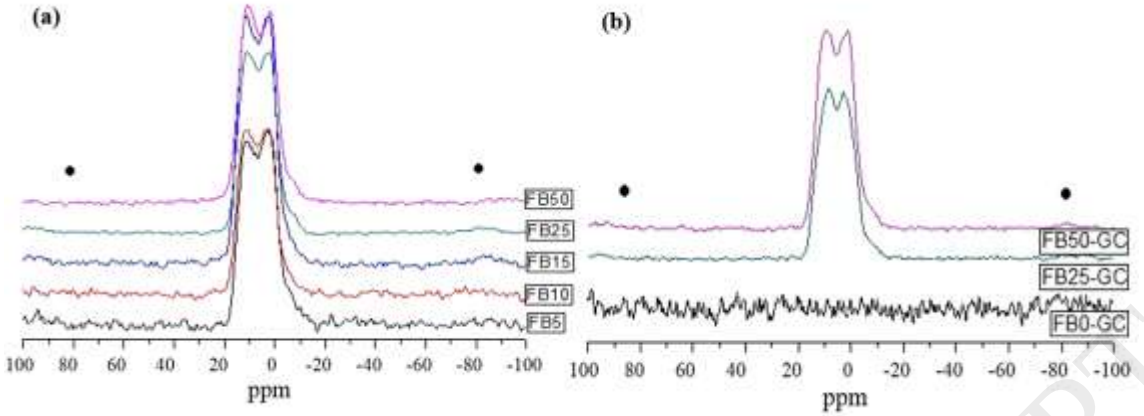

Figure 5: ^{11}B MAS-NMR spectra of different boron-substituted (a) glasses and (b) glass-ceramics. Spinning bands are marked with ●.

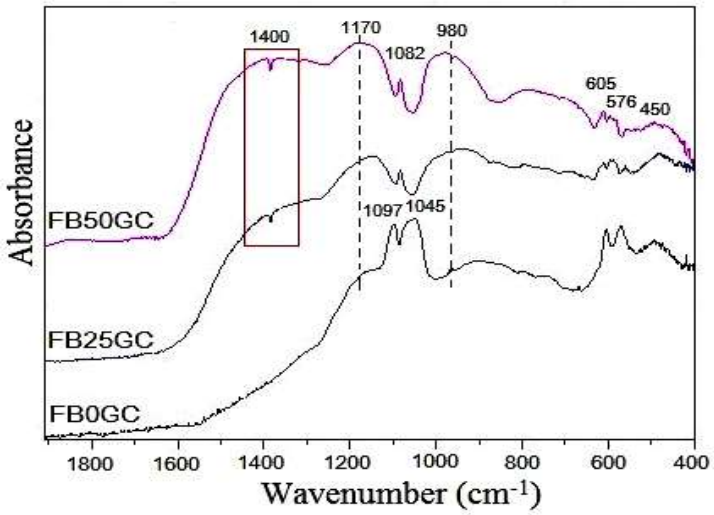

Figure 6: FTIR spectra of boron-substituted glass-ceramics.

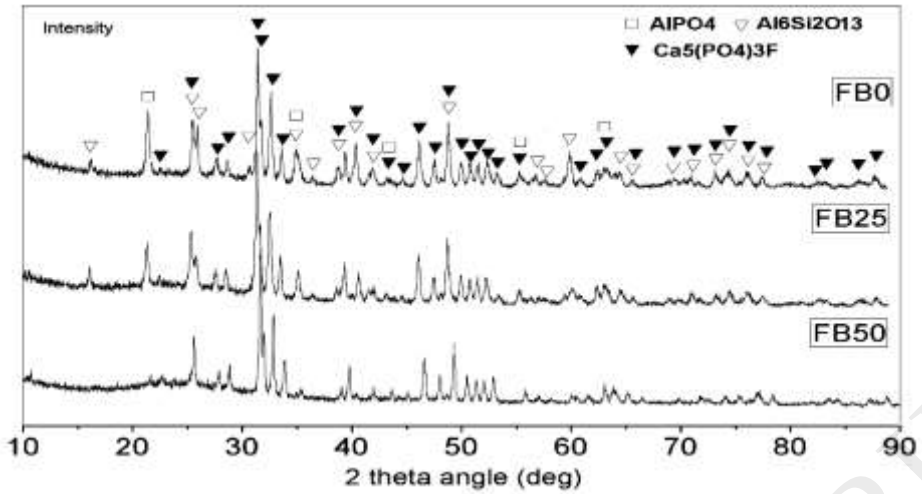

Figure 7: X-ray powder diffraction spectra of heat-treated (1100°C), boron-substituted fluorine-containing glass-ceramics. The heat-treated FB0 glass spectrum is presented as reference material. □ = aluminium phosphate, ▼= fluorapatite, ▽ = mullite.

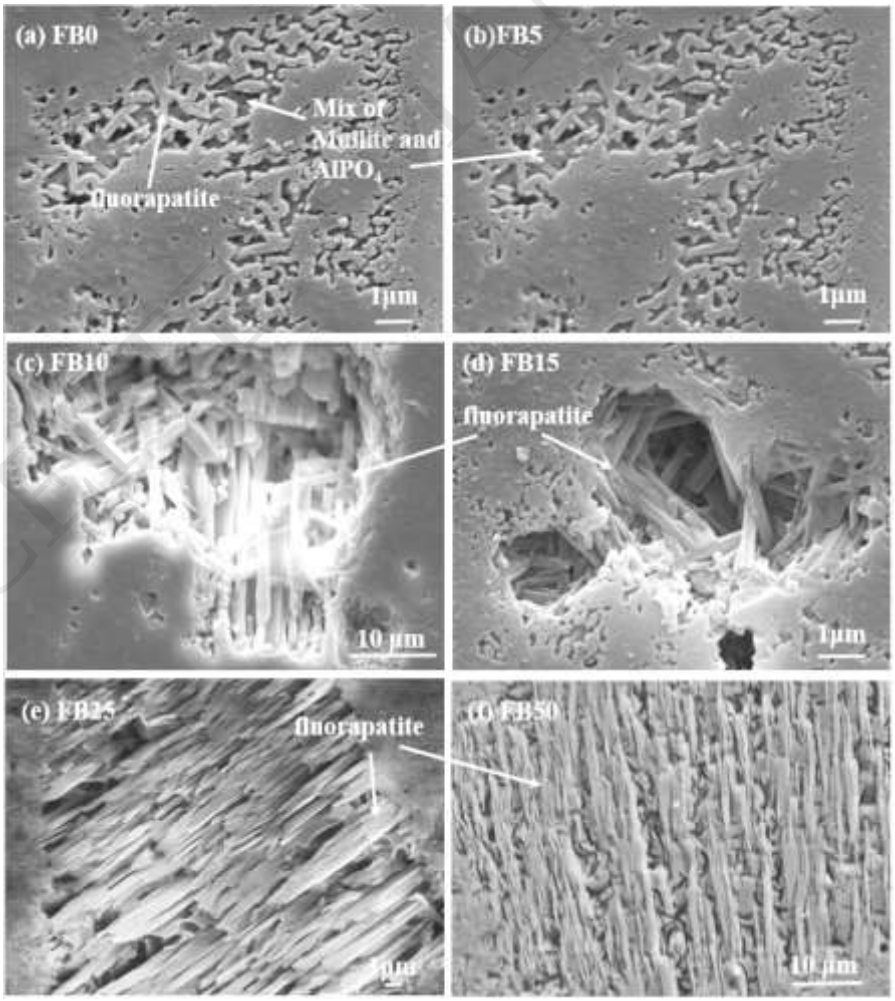

Figure 8: SEM morphologies of glass-ceramics, (a) FB0, (b)FB5, (c)FB10, (d)FB15, (e)FB25 and (f)FB50.

Table 1: Molar composition of boron-substituted fluoro-aluminosilicate glasses.

Glass code	SiO_2	Al_2O_3	P_2O_5	CaO	CaF_2	B_2O_3
FB0	4.5	3	1.5	3	2	0
FB5	4.5	2.85	1.5	3	2	0.15
FB10	4.5	2.7	1.5	3	2	0.3
FB15	4.5	2.55	1.5	3	2	0.45
FB25	4.5	2.25	1.5	3	2	0.75
FB50	4.5	1.5	1.5	3	2	1.5

Table 2: DSC analysis data of T_g, T_{p1} and T_{p2} for all boron-substituted glasses measured at a heating rate of 10^{o}C/min (molar %).

Glass	Boron substitution	T_g(^{o}C)	T_{p1}(^{o}C)	T_{p2}(^{o}C)	T_{p3}(^{o}C)
FB0	0	653±6	741±12	1053±20	-
FB5	5	647±6	728±11	977±18	-
FB10	10	656±5	718±12	1014±18	-
FB15	15	648±5	704±11	1089±19	-
FB25	25	605±6	636±10	715±18	946±27
FB50	50	630±7	643±12	763±17	-

Table 3: MAS-NMR spectroscopy on boron-substituted fluoro-aluminosilicate glasses and glass-ceramics (^{11}B, ppm).

Glass	FB0	FB5	FB10	FB15	FB25	FB50
chemical shift	-	0.8 ; 9.0	0.8 ; 9.5	0.4 ; 9.5	0.2 ; 9.4	0.2 ; 9.3

Glass-ceramic	FB0				FB25	FB50
chemical shift	-	-	-	-	1.6 ; 7.0	-0.3 ; 7.9

Table 4: Chemical composition of glass-ceramic phases in EDX analysis (±1 at%).

	Si	Al	Ca	P	F	O
Bright phase	2.27	2.58	14.38	9.42	11.19	60.15
Dark phase	16.81	20.20	6.94	3.41	2.48	50.16